Particle-hole symmetry and transport properties of the flux state in underdoped cuprates

Masaru Onoda[1,*] and Naoto Nagaosa[1,2,†]
[1]*Correlated Electron Research Center (CERC), National Institute of Advanced Industrial Science and Technology (AIST), Tsukuba Central 4, Tsukuba 305-8562, Japan*
[2]*Department of Applied Physics, University of Tokyo, Bunkyo-ku, Tokyo 113-8656, Japan*
(Received 13 December 2001; published 17 May 2002)

Transport properties, i.e., conductivities $\sigma_{\mu\nu}$, Hall constant R_H, and thermopower S are studied for the flux state with the gauge flux ϕ per plaquette, which may model the underdoped cuprates, with the emphasis on the particle-hole and parity/chiral symmetries. This model is reduced to the Dirac fermions in (2+1)D, (where D means dimensional) with a mass gap introduced by the antiferromagnetic (AF) long-range order and/or the stripe formation. Without the mass gap, the Hall constant R_H and the thermopower S obey the two-parameter scaling laws, $R_H \cong a^2/|e| x f_{R_H}(t\sqrt{x}/k_BT, \hbar/\tau k_BT)$ and $S \cong k_B/|e| f_S(t\sqrt{x}/k_BT, \hbar/\tau k_BT)$, with a being the lattice constant, x the hole concentration, and τ the transport lifetime. The R_H and S show the strong temperature dependence due to the recovery of the particle-hole symmetry at high temperatures. The x dependences of $\sigma_{xx}(\propto \sqrt{x})$ and σ_{xy} (independent of x) are in a sharp contradiction with the experiments. Therefore, there is no signature of the particle-hole symmetry or the massless Dirac fermions in the underdoped cuprates even above the Neel temperature T_N. With the mass gap introduced by the AF order, there occurs the parity anomaly for each of the Dirac fermions. However the contributions from different valleys and spins cancel each other to result in no spontaneous Hall effect even if the time-reversal symmetry is broken with $\phi \neq \pi$. The effects of the stripes are also studied. The diagonal and vertical (horizontal) stripes have quite different influence on the transport properties. The suppression of R_H occurs at low temperature only when (i) both the AF order and the vertical (horizontal) stripe coexist, and (ii) the average over the in-plane direction is taken. Discussions on the recent experiments are given from the viewpoint of these theoretical results.

DOI: 10.1103/PhysRevB.65.214502 PACS number(s): 74.25.Fy, 74.72.−h, 71.10.Fd, 72.15.Eb

I. INTRODUCTION

Since the discovery of high-T_c cuprates, intensive studies have been done on the two-dimensional (2D) antiferromagnets. It is now established that the ground state of the 2D Heisenberg antiferromagnet with the nearest-neighbor interaction on the square lattice shows an antiferromagnetic (AF) long-range ordering at zero temperature,[1] and the low energy spin excitation can be described in terms of the spin-wave theory. However this does not mean that the electronic state in the antiferromagnets is fully understood. Compared with the triplet channel of the two-particle correlation functions, the single particle properties such as the angle-resolved photoemission spectra (ARPES),[2] and the singlet channel correlation functions such as the charge transport properties[3–8] still remain controversial. In fact, there are two different pictures for it. One is the conventional spin-density-wave (SDW) picture[9] with the wave number $\vec{Q}=(\pi,\pi)$, where both the weak- and strong-coupling regions can be smoothly connected. The other picture is the π-flux state[10] originated from the resonating valence bond (RVB) idea.[11] At half filling, the π-flux state is equivalent to the d-wave singlet paring state[12,13] due to the particle-hole SU(2) symmetry.[14] The Gutzwiller projected wave function with the d-wave paring and AF orders gives a better energy compared with that only with the AF order.[15] Also the higher-energy continuum of the neutron-scattering spectra and Raman-scattering spectra has been analyzed in terms of this π-flux state.[15]

The dispersion of a single hole put into this antiferromagnet is an important issue studied intensively in terms of the self-consistent Born approximation,[16] exact diagonalization,[17] spinon-holon bound-state picture,[18] and variational method[19]. Using the t-J model, all the analyses give the maximum of the hole dispersion at $\vec{k}=(\pm\pi/2, \pm\pi/2)$. This dispersion can be understood in terms of the π-flux picture,[18,19] which introduces the nodal Fermi points of the spinons at $\vec{k}=(\pm\pi/2,\pm\pi/2)$ with the dispersion similar to the d-wave superconductors. This fits the ARPES experiments in the undoped cuprates.[2]

At finite doping, the slave-boson mean-field theory of the t-J model predicts the state with both the singlet RVB and AF orders for small x.[20] The SU(2) symmetry has been employed to represent the constraint and the underdoped pseudogap region is characterized as the staggered flux state with spin-charge separation,[21] which can be regarded as the fluctuating state between the d-wave pairing state and the current order state. On the other hand, the staggered flux state with the electron coordinates with the real current ordering and periodicity doubling has been proposed for the underdoped cuprates.[22]

Recently there appeared several experiments on the Hall coefficient R_H and the thermopower S in the heavily underdoped cuprates, which raised the issue of particle-hole symmetry.[6–8] The R_H as well as the S show a strong suppression below the Neel temperature T_N in some YBCO samples,[6] while this is not the case for other samples.[7] This strongly suggests that the transport properties below T_N are sensitive to the oxygen chain ordering and/or the self-organization of electrons such as the stripes, which depends on the annealing procedure in the sample preparation. An-

other interesting clue is that in LSCO the suppression of the Hall effect is observed only in the vertical (horizontal) stripe state and not in the diagonal stripe state for $x<0.05$.[23,24] Above T_N, R_H is a decreasing function of temperature, which remains one of the most puzzling features in the normal-state properties.[3,5,25,6]

In the SDW picture, a large metallic Fermi surface enclosing the area of $1-x$ (x: hole concentration) is recovered above T_N. Therefore we expect the drastic change of the Hall constant from $R_H=-a^2/(1-x)$ to $R_H=a^2/x$ when the temperature T is lowered across T_N. (Here a is the lattice constant.) Correspondingly the resistivity should be affected by the onset of the AF order. This is in sharp contradiction with the experiments. Even above T_N, the system behaves as the doped Mott insulator with the small number of holes,[3,5,6] and even a slight change of the resistivity is not observed at T_N.[7]

Considering all these clues, it is worthwhile to study the transport properties of the slightly doped π-flux state both above and below T_N, which we undertake in this paper. We will neglect the interactions between electrons and the disorder potentials. The former is justified because the quasiparticle number is small at low temperature due to the reduced density of states and the e-e interaction is irrelevant. The latter becomes important at low temperature for small x where the resistivity shows an upturn, but is irrelevant for the temperature and x range of our interest. We also study the effect of the stripe formation on the Hall constant and the thermopower, and show that oxygen chain ordering is crucial for these quantities. The deviation of the flux from π, which breaks the time-reversal symmetry and produces current ordering, is also studied. This issue is closely related to the parity anomaly[26] in (2+1)D because the two species of the Dirac fermions acquire a mass gap due to the AF ordering. Therefore the undoped and underdoped cuprates offer an interesting laboratory to study the transport properties of the Dirac fermions with nontrivial topological nature influenced by the AF order and/or the stripe formation. The Dirac fermion has been studied also in the context of the nodal quasiparticle in the d-wave supercouductors.[27] In this case the Fermi energy is always at $E=0$ and the particle-hole symmetry remains. Under the external magnetic field H, the formation of the vortex lattice is crucial, which introduces the magnetic length scale $\ell_H\sim H^{-1/2}$. In the present case, on the other hand, there occurs no Meissner effect, and one can see the response of the Dirac fermions in the uniform state, while the particle-hole symmetry is broken due to the shift of the Fermi energy from $E=0$. This introduces the length scale $\ell_x\sim x^{-1/2}$, i.e., the interhole distance, and we can have a new kind of scaling when neither AF ordering nor the stripe formation occur.

The plan of this paper follows. In Sec. II, our model Hamiltonian is introduced and its spectrum under the external magnetic field is reviewed. In Sec. III, the electromagnetic and thermal responses are studied for the Dirac fermions without stripes. The effects of the stripes are studied in Sec. IV, and Sec. V is devoted to discussions in comparison with experiments.

II. HAMILTONIAN

We start with the most generic Hamiltonian in the staggered flux state with anti-ferromagnetic and stripe (quasi-)order, which are treated as on-site potentials in the mean-field theory. Hereafter, we take the units in which $\hbar=c=1$.

$$H=-\sum_{\langle\vec{r},\vec{r}'\rangle,\sigma} t_{\vec{r},\vec{r}'}c^{\dagger}_{\vec{r}\sigma}c_{\vec{r}'\sigma}-\sum_{\vec{r},\sigma}[\mu+u_\sigma\cos(\vec{Q}\cdot\vec{r}) +v\cos(\vec{Q}_v\cdot\vec{r})]c^{\dagger}_{\vec{r}\sigma}c_{\vec{r}\sigma}. \tag{1}$$

The transfer integral $t_{\vec{r}\pm\hat{x},\vec{r}}=t^{*}_{\vec{r}\pm\hat{y},\vec{r}}=te^{i\phi/4}$ (with $r_x+r_y=$even) represents the staggered flux ϕ for each plaquette. In the RVB picture, ϕ is generated by the superexchange interaction J and equals π in the undoped case. Therefore, in our representation, the transfer integral t is estimated as $t\cong 0.8J$, and should not be confused with t in the t-J model.[18] In the second term, u_σ is the mean-field potential for the σ spin electrons with the wave number $\vec{Q}=(\pi,\pi)$, which originates from the AF order m_{AF} and/or the diagonal stripe formation $m_{\rm diag}$ as $u_\sigma=\sigma m_{AF}+m_{\rm diag}$, while v is that from the vertical stripe formation with $\vec{Q}_v=(\pi,0)$. This is the result of the higher-order process in the stripe potential with the wave number $\vec{Q}_{\rm stripe}=(\pi/M,\pi/M)$ (diagonal case) or $\vec{Q}_{\rm stripe}=(\pi/M,0)$ (vertical case). The chemical potential μ is zero at the half-filling. The eigenvalues for each $\vec{k}$ are

$$\epsilon_\sigma(\vec{k})=\pm\left[4t^2(\cos^2k_x+\cos^2k_y)+u_\sigma^2+v^2\pm 2\sqrt{\left(4t^2\cos\frac{\phi}{2}\cos k_x\cos k_y\right)^2+v^2(4t^2\cos^2k_y+u_\sigma^2)}\right]^{1/2}. \tag{2}$$

First, we consider the case without the vertical stripe. In this case, the low-energy electronic states are described in terms of the two Dirac fermions at $\vec{k}_1=(\pi/2,\pi/2)$ and $\vec{k}_2=(\pi/2,-\pi/2)$, which we call sector 1 and 2, respectively. Measuring the momenta from these $\vec{k}_{1,2}$ points, and in the continuum approximation the Hamiltonian is given as

$$H_{\rm eff}=\sum_{i,\sigma}\int d^2r\,\psi^{\dagger}_{i\sigma}(\vec{r})\hat{\mathcal{H}}_{i\sigma}\psi_{i\sigma}(\vec{r}), \tag{3}$$

where $\psi^{(\dagger)}_{i\sigma}(\vec{r})$ is the annihilation (creation) operator of i sector ($i=1,2$) with σ spin,

$$\hat{\mathcal{H}}_{1\sigma}=\begin{bmatrix} u_\sigma-\mu & 2ta(\hat{p}_x+e^{-i\phi/2}\hat{p}_y) \\ 2ta(\hat{p}_x+e^{i\phi/2}\hat{p}_y) & -u_\sigma-\mu \end{bmatrix}, \quad (4)$$

and $\hat{\mathcal{H}}_{2\sigma}=\hat{\mathcal{H}}_{1\sigma}|_{\substack{u_\sigma\to -u_\sigma \\ \phi\to 2\pi-\phi}}$. Here $\hat{p}_\mu=-i\partial_\mu$ and a is the lattice constant. As is evident from the above Hamiltonian, each Dirac fermion has a mass term with positive or negative sign, and shows the parity anomaly.[26] When the external electromagnetic field A_μ is coupled to each Dirac fermion, the Chern-Simons term $\varepsilon^{\mu\nu\lambda}A_\mu\partial_\nu A_\lambda$ is generated. Therefore the Dirac fermion with positive (negative) u_σ has the right (left) chirality. Because there are two right (R) and left (L) Dirac fermions, there occurs the cancellation of the Chern-Simons terms, and no spontaneous Hall effect results. This remains true even when the flux ϕ is different from π and the time-reversal symmetry is broken to produce the current order. It is because the current pattern is staggered, and does not affect the uniform response in an essential way.

Now we briefly review the Dirac fermions in the presence of the external uniform magnetic field B, which can be analytically solved.[28,29] In the effective theory represented by Eq. (3), the first-quantized Hamiltonian Eq. (4) is rewritten by the replacement, $\hat{p}_\mu\to\hat{\pi}_\mu=\hat{p}_\mu-eA_\mu(\vec{r})$, where $[\vec{\nabla}\times\vec{A}(\vec{r})_z=B$. Then we define the following bosonic operators as

$$\hat{a}_\phi=\frac{1}{\sqrt{2|eB_\phi|}}[\hat{\pi}_x+e^{i\,\mathrm{sgn}(eB_\phi)\phi/2}\hat{\pi}_y], \quad (5)$$

$$\hat{a}_\phi^\dagger=\frac{1}{\sqrt{2|eB_\phi|}}[\hat{\pi}_x+e^{-i\,\mathrm{sgn}(eB_\phi)\phi/2}\hat{\pi}_y]. \quad (6)$$

These operators satisfy the commutation relation $[\hat{a}_\phi,\hat{a}_\phi^\dagger]=1$. Using these operators and the Pauli matrices τ_i, $(i=1,2,3)$, Eq. (4) is rewritten as

$$\hat{\mathcal{H}}_{1\sigma}=\frac{K_{eB_\phi}}{2}[(\hat{a}_\phi+\hat{a}_\phi^\dagger)\tau_1-i\,\mathrm{sgn}(eB_\phi)(\hat{a}_\phi-\hat{a}_\phi^\dagger)\tau_2]+u_\sigma\tau_3-\mu I. \quad (7)$$

The eigenvector $(n\geqslant 1)$ is

$$|n\sigma\pm\rangle=\frac{1}{\sqrt{2\epsilon_n}}[\sqrt{\epsilon_n\pm\mathrm{sgn}(eB_\phi)u_\sigma}|n\rangle\otimes|\tilde{\uparrow}\rangle \pm\sqrt{\epsilon_n\mp\mathrm{sgn}(eB_\phi)u_\sigma}|n-1\rangle\otimes|\tilde{\downarrow}\rangle]\otimes|\sigma\rangle, \quad (8)$$

with the eigenvalue $\pm\epsilon_{n\sigma}$ being given by

$$\epsilon_{n\sigma}=\sqrt{K_{eB_\phi}^2 n+u_\sigma^2}, \quad (9)$$

$$K_{eB_\phi}=\sqrt{8t^2a^2|eB_\phi|}, \quad B_\phi=B\sin\frac{\phi}{2}. \quad (10)$$

Here $|n\rangle$ is the eigenvector of $\hat{a}_\phi^\dagger\hat{a}_\phi$ with the eigenvalue n, $|\tilde{\uparrow}(\tilde{\downarrow})\rangle$ is the eigenvector of $\mathrm{sgn}(eB_\phi)\tau_3$ with the eigenvalue $+1(-1)$, and the quantum index for the intralevel orbitals is omitted. $|\tilde{\uparrow}(\tilde{\downarrow})\rangle$ should not be confused with a real-spin eigenvector $|\sigma\rangle$, but it comes from the two-component nature of a Dirac fermion. Especially, the zero mode is given by

$$|0\sigma\pm\rangle=\tfrac{1}{2}[1\pm\mathrm{sgn}(u_\sigma eB_\phi)]|0\rangle\otimes|\tilde{\uparrow}\rangle\otimes|\sigma\rangle. \quad (11)$$

Therefore, there exists only one zero mode $|0\sigma+\rangle$ or $|0\sigma-\rangle$ for each sector and its energy is $\epsilon_{0\sigma}=|u_\sigma|$ or $-|u_\sigma|$ depending on the direction of the external magnetic field B and the chirality of Dirac fermions. We can also define effective current operators as follows: $\hat{j}_x=2ta\tau_1$ and $\hat{j}_y=2ta(\cos\phi/2\tau_1+\sin\phi/2\tau_2)$.

III. ELECTROMAGNETIC AND THERMAL RESPONSES

The electromagnetic and thermal linear response functions are obtained by the Kubo formula. We put the above solutions into the Kubo formula for $\sigma_{\mu\nu}(\omega)$ and approximate the effect of the relaxation by replacing ω by $\omega+i/\tau$ with the lifetime τ. This approximation reproduces the Drude formula for $\sigma_{\mu\nu}(\omega)$ in the simplest case. The contribution from sector 1 with σ spin is presented in Appendix A. The total conductivity is given by summing up the contribution from all sectors. This procedure makes anomalous terms, which come from the interband effect, cancel out with each other, and lead to the consistent result in the AF ordered state, i.e., no parity symmetry breaking in the limit $B\to 0$.

Equations (A5) and (A6) are valid for general cases including both the quantum limit ($\tau\to\infty$ with finite B) and the semiclassical limit ($K_{eB_\phi}\tau\ll 1\ll|\mu|\tau$). In the former case, Eqs. (A5) and (A6) represent the integer quantum Hall effect, while in the latter case they correspond to the usual Hall effect. In the latter case, we obtain the same formula with that given by the Boltzmann equation. For example, with only the AF order and at low temperature, Eqs. (A5) and (A6) lead to

$$\sigma_{xx}\cong\frac{e^2}{2\pi}\frac{8\pi xt^2\tau}{\sqrt{4\pi xt^2\left|\sin\frac{\phi}{2}\right|+m_{AF}^2}}, \quad (12)$$

$$\sigma_{xy}\cong\frac{e^2}{2\pi}\frac{(8\pi xt^2\tau)^2}{4\pi xt^2\left|\sin\frac{\phi}{2}\right|+m_{AF}^2}\frac{a^2|e|B}{2\pi x}\sin^2\frac{\phi}{2}, \quad (13)$$

and the Hall coefficient R_H is given by

$$R_H\cong\frac{\sigma_{xy}}{B\sigma_{xx}^2}\cong\frac{a^2}{|e|x}\sin^2\frac{\phi}{2} \quad (14)$$

independent of the presence/absence of the AF order. This is

reduced to the conventional result $R_H = a^2/(|e|x)$ for the hole system with concentration x when we put $\phi = \pi$. However the x dependences of σ_{xx} and σ_{xy} are peculiar in the absence of the AF order, namely, $\sigma_{xx} \propto \sqrt{x}$ and σ_{xy} being independent of x when we neglect the x dependence of τ. These are understood as follows. The σ_{xx} is proportional to the density of states at the Fermi energy, which is proportional to $\sqrt{x}$ for the massless Dirac fermion. As for σ_{xy}, on the other hand, the geometric interpretation is useful.[30] The Hall conductivity is determined by the scattering path length, $\vec{l}(\vec{k}) = \tau \vec{\nabla} \epsilon(\vec{k})$, which is independent of the magnitude $|\vec{k}|$ for linear dispersion and hence σ_{xy} is independent of x. In Eq. (A6), this behavior is the consequence of the dominant contribution from the zero mode of the Dirac fermions to σ_{xy}. On the other hand, when $\sqrt{4\pi x t} \ll |m_{AF}|$, the usual dispersion $\epsilon(\vec{k}) \propto \vec{k}^2$ is relevant and the usual x dependences, $\sigma_{xx} \propto x$ and $\sigma_{xy} \propto x$ result. The thermopower S at a sufficiently low temperature is also obtained in a similar way as

$$S \cong \frac{k_B}{|e|} \frac{\pi^2}{3} k_B T \frac{4\pi x t^2 \left| \sin \frac{\phi}{2} \right| + 2m_{AF}^2}{4\pi x t^2 \left| \sin \frac{\phi}{2} \right| \left[4\pi x t^2 \left| \sin \frac{\phi}{2} \right| + m_{AF}^2 \right]^{1/2}}. \tag{15}$$

The x dependence of S is also peculiar in the absence of the AF order, i.e., $S \propto 1/\sqrt{x}$.

Next we consider the temperature dependence of R_H and S, which originates from the Fermi distribution function $f_F(T, \epsilon, \mu(T))$. Here the energy is averaged over $\sim k_B T$, and both the particle and hole branches contribute with the opposite signs to R_H and S when $k_B T > |\mu(T)|$. Furthermore, $|\mu(T)|$ is a decreasing function of temperature as presented in Appendix B. For example, when $m_{AF} = 0$, it behaves at $k_B T \ll O(t\sqrt{x})$

$$|\mu(T)| \cong \sqrt{4\pi x t^2 \left| \sin \frac{\phi}{2} \right| - \frac{\pi^2}{3} (k_B T)^2}, \tag{16}$$

and at $k_B T \gg O(t\sqrt{x})$

$$|\mu(T)| \cong \frac{\pi x t^2}{\ln 2} \left| \sin \frac{\phi}{2} \right| \frac{1}{k_B T}. \tag{17}$$

Therefore, as long as the flux order is present, the particle-hole symmetry is approximately restored at high temperatures even in the doped system, and both R_H and S are reduced as shown in Figs. 1(a) and 1(b), which are the results of the original lattice model. The peak in R_H occurs because the suppression of σ_{xx} as increasing T dominates at low temperature. After all, a low carrier density and a narrow gap result in these features, i.e., having a peak at moderate temperature and decreasing at high temperature. It is worthwhile to note that the temperature dependence of S resembles those of rare-earth compounds, such as YbCuAl, which have low carrier densities and narrow gaps.[31]

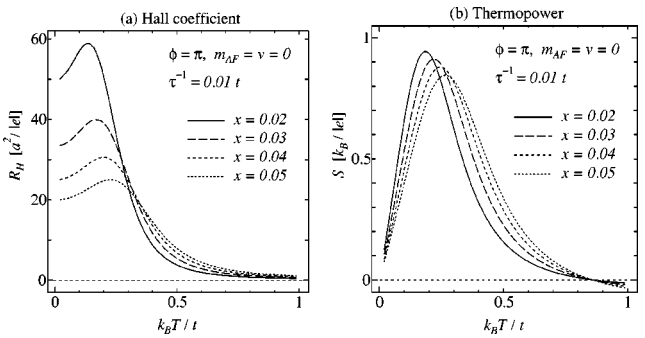

FIG. 1. Temperature dependences of (a) the Hall coefficient R_H in the unit $a^2/|e|$, and (b) the thermopower S in the unit $k_B/|e|$ for $m_{AF} = v = 0$.

In the case of $m_{AF} = 0$ and the limit $B \to 0$, the following scaling laws are expected by the continuum model

$$R_H = \frac{a^2}{|e|x} f_{R_H}\left(\frac{t\sqrt{x}}{k_B T}, \frac{1}{\tau k_B T} \right), \tag{18}$$

$$S = \frac{k_B}{|e|} f_S\left(\frac{t\sqrt{x}}{k_B T}, \frac{1}{\tau k_B T} \right), \tag{19}$$

where f_{R_H} and f_S are dimensionless functions. (The details are given in Appendix C.) The dependence on $t\sqrt{x}/(k_B T)$ is because of $\mu/(k_B T)$ being a dimensionless function of $t\sqrt{x}/(k_B T)$, and the dependence on $\tau k_B T$ comes from the transition between the highest valence band and the lowest conduction band. The latter is neglected in the Boltzmann transport theory. In a physical sense, the contribution from transitions between two bands would be very small when the condition $1 \ll |\mu|\tau$ is satisfied, i.e., in the semiclassical limit. In this case, we get the one-parameter scaling laws

$$R_H \cong \frac{a^2}{|e|x} f_{R_H}\left(\frac{t\sqrt{x}}{k_B T} \right), \quad S \cong \frac{k_B}{|e|} f_S\left(\frac{t\sqrt{x}}{k_B T} \right). \tag{20}$$

Therefore, both xR_H and S are expected to scale as functions of $t\sqrt{x}/(k_B T)$. Figures 2(a) and 2(b) show the scaling behav-

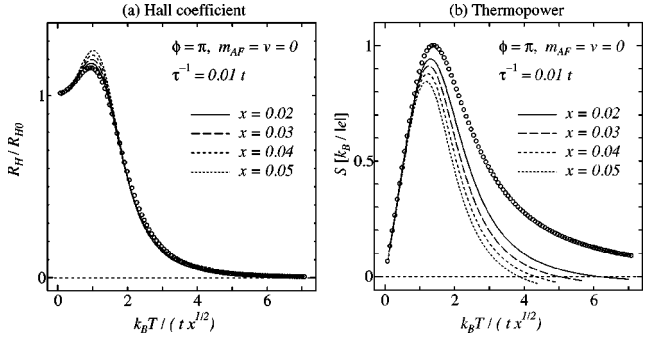

FIG. 2. Scaling of temperature dependences of (a) the Hall coefficient R_H divided by $R_{H0} = a^2/(|e|x)$, and (b) the thermopower S in the unit $k_B/|e|$ for $m_{AF} = v = 0$. The open circles are scaling functions calculated in the continuum model.

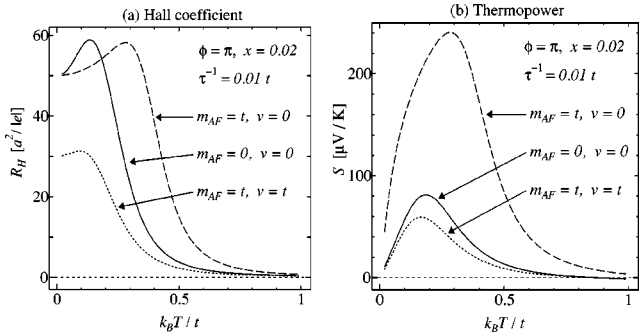

FIG. 3. Temperature dependences of (a) the Hall coefficient R_H in the unit $a^2/|e|$, and (b) the thermopower S in the unit μV/K for $(m_{AF},v)=(0,0)$, $(t,0)$, and (t,t).

iors of R_H and S given in Figs. 1(a) and 1(b). We can see that the single-parameter scaling law of R_H works fairly well in a broad temperature range. On the other hand, for S, it works only at low temperatures. This is because S contains the energy integral that has one more energy dimension than the integral for R_H, and S is more sensitive to the higher-energy region where the lattice structure is relevant.

In Figs. 3(a) and 3(b), the temperature dependences of R_H and S are shown in the presence of the AF order and the vertical (horizontal) stripe. These results are obtained for the lattice model in terms of the Boltzmann transport theory where the interband effect is neglected. We can observe that the AF order (without the stripe formation) results in the enhancement of R_H and S. One reason of this enhancement is that the AF order suppresses the recovery of the particle-hole symmetry at high temperatures. (The details are given in Appendix B.) Another reason is that the heavier mass m_{AF} makes the conductivity smaller as seen in Eqs. (12) and (13). The former reason is crucial both for R_H and S. On the other hand, the latter would be crucial only for S as expected from the comparison of Eqs. (14) and (15). This is because the explicit dependence of σ_{xx} and σ_{xy} on m_{AF} nearly cancel each other in R_H. Therefore, the enhancement of S is more drastic than that of R_H. As for the effect of the stripe, we will consider it closely in the following section.

IV. EFFECT OF STRIPE FORMATION

The quasi-one-dimensional spin/charge ordering occurs in some cuprates,[32] and consequently affects the transport properties.[7,8,23] Therefore it is worthwhile to study the effect of the stripe formation on the flux state. Some works have been done assuming the one dimensionality, which corresponds the limit of strong stripe potential.[33] In this section, we give an alternative and complementary study starting from the 2D flux state. It is easy to see that the effects of the stripes are essentially different between the diagonal and vertical (horizontal) ones, because the vertical (horizontal) stripe introduces the off-diagonal matrix elements between the two Dirac fermions around $\vec{k}_1$ and $\vec{k}_2$, while the diagonal one does not. Therefore the effect of the diagonal stripe is similar to that of the AF order and we do not expect any drastic change of R_H in the case of the diagonal stripe, although it makes the mass gaps of different spins unbalanced and leads to the modification of S. It is noted that the change of the mass gap modifies S as in Eq. (15). (The unbalance of the mass gaps of different spins also leads to the ferrimagnetism.) After all, the drastic modifications of both R_H and S are expected only when the vertical (horizontal) stripe formation occurs. We will focus on this case below.

In the presence of the stripe, there appears the anisotropy in the plane. A naive expectation is that the 1D nature of the transport along the stripe reduces R_H. However, this is not the case, because the stripe does suppress not only σ_{xy} but also one of σ_{xx} and σ_{yy} with $R_H \cong \sigma_{xy}/(B\sigma_{xx}\sigma_{yy})$ being unchanged. This is the case also in our explicit calculation showing that $R_H = a^2/(|e|x)$ is a robust feature at a low temperature. At this point, we must consider the configuration of the stripe in cuprates. When there are stripes, their direction would be different in each CuO_2 layer as in LSCO, or there are domains of stripes with different directions in a layer as in twined YBCO. In the former system, we simply assume that the vertical and horizontal types occur alternately. Then it is reasonable to average the contributions from different layers, because they can be regarded as a *parallel* circuit, i.e. we should take an average of conductivity tensor not of resistivity tensor. Also in the latter system, more conductive regions percolate and hence dominate the conductivity of the system. Therefore it is reasonable to take average of σ_{xx} and σ_{yy}. Then the observed R_H is suppressed because only σ_{xy} is reduced considerably while $\sigma=(\sigma_{xx}+\sigma_{yy})/2$ is not, and $R_H \cong \sigma_{xy}/(B\sigma^2)$ is suppressed.

Before discussing general cases, we consider some special cases where R_H and S can be analytically evaluated at a low temperature by the Boltzmann equation. The first limiting condition is that $|m_{AF}|$ is sufficiently larger than the kinetic energy $O(t\sqrt{x})$. The second condition is $|v| \ll |m_{AF}|$ or $\sqrt{4t^2+m_{AF}^2} \ll |v|$. With these conditions, the low-energy physics would be approximately described by quasiparticles of linear dispersions at $\vec{k}=(\pi/2,\pi/2)$ and $(\pi/2,0)$, respectively. It is noted here that these quasiparticles are not simple two-component Dirac fermions, because the vertical stripe formation mixes the two-component Dirac fermions with different chiralities as mentioned above. For the case $|v| < |v_c| \sim 2\pi x t^2/m_{AF}$, the analysis is complicated because we should consider two bands doped in different ways. It is noted here that there are two upper bands and two lower bands for each spin degree of freedom when $m_{AF} \neq 0$ and $v \neq 0$. The analysis of R_H in this case is given in Appendix E. When $|v|$ is larger than the critical value $|v_c|$, only the second band is doped. Therefore, for $|v_c| < |v| \ll |m_{AF}|$ or $\sqrt{4t^2+m_{AF}^2} \ll |v|$, the result is expressed as

$$R_H \simeq \frac{a^2}{|e|x} \frac{4t^2\tilde{t}^2}{(t^2+\tilde{t}^2)^2}, \tag{21}$$

where $\tilde{t} = t\sqrt{1-|v/m_{AF}|}$ for $|v_c| < |v| \ll |m_{AF}|$, or $\tilde{t} = t\sqrt{|v|/\sqrt{4t^2+m_{AF}^2}-1}$ for $\sqrt{4t^2+m_{AF}^2} \ll |v|$.

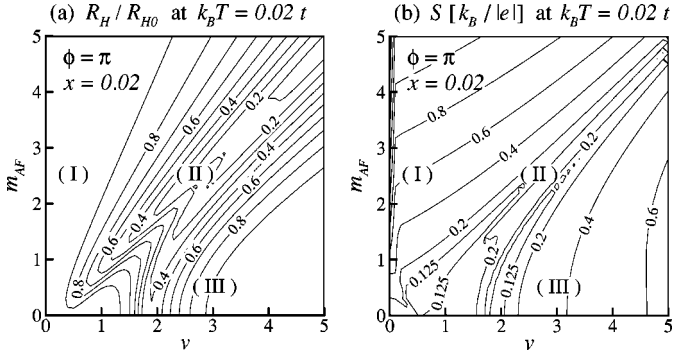

FIG. 4. (a) Hall coefficient R_H divided by $R_{H0}=a^2/(|e|x)$, and (b) thermopower S in the unit $k_B/|e|$. Symbols (I), (II), and (III) correspond to Figs. 5(a), 5(b), and 5(c).

On the other hand, the thermopower $S_\mu \sim \beta\langle J^e_\mu J^e_\mu\rangle^{-1}\langle J^e_\mu J^Q_\mu\rangle$, where $\vec{J}^e$ is the electric current density and $\vec{J}^Q$ is the heat current density, along the direction $\mu = x,y$ remains almost isotropic because the anisotropy of the correlation functions $\langle J^e_\mu J^e_\mu\rangle$ and $\langle J^e_\mu J^Q_\mu\rangle$ cancels each other in the numerator and denominator, respectively. However, S is rather sensitive to the change of the gap and the electronic dispersion, because $\langle J^e_\mu J^Q_\mu\rangle$ contains additional dimension of energy and is suppressed by the coexistence of the AF order and vertical (horizontal) stripe. For the case $|v_c|<|v| \ll |m_{AF}|$ or $\sqrt{4t^2+m_{AF}^2} \ll |v|$, it is given at a low temperature by

$$S \simeq \frac{k_B}{|e|}\frac{\pi^2}{3}k_B T \frac{8\pi x t\tilde{t}+2\tilde{m}^2}{8\pi x t\tilde{t}[8\pi x t\tilde{t}+\tilde{m}^2]^{1/2}}, \qquad (22)$$

where $\tilde{t}=t\sqrt{1-|v/m_{AF}|}$ and $\tilde{m}=|m_{AF}|-|v|$ for $|v_c|<|v| \ll |m_{AF}|$, or $\tilde{t}=t\sqrt{|v|/\sqrt{4t^2+m_{AF}^2}-1}$ and $\tilde{m}=|v| - \sqrt{4t^2+m_{AF}^2}$ for $\sqrt{4t^2+m_{AF}^2} \ll |v|$. Comparing Eq. (15) in the case $\phi=\pi$ and Eq. (22), we can see that the weak stripe, i.e., $|v|\sim|v_c|$, strongly suppresses the thermopower with sufficiently strong AF order, i.e., large $|m_{AF}|$. Therefore a crucial test of this scenario is to measure the thermopower S in the untwined sample where R_H is not suppressed.

Now let us turn to the results for R_H and S in general cases. Although the analytic results for R_H [Eq. (21)] and S [Eq. (22)] are valid only in the limiting cases, they show what are crucial for each quantity. As for R_H, the anisotropy of the transfer integral, i.e., the anisotropy of the velocity, is crucial with the help of the averaging of the conductivity tensor. On the other hand, as for S, the mass reduction, i.e., the reduction of the band gap, is also crucial as is the anisotropy of the transfer integral. Therefore, interesting results are expected in the nontrivial case $|m_{AF}| \lesssim |v| \lesssim \sqrt{4t^2+m_{AF}^2}$, because the energy dispersion is highly anisotropic and there is no band gap between the two middle bands. We employ the Boltzmann transport theory and numerically evaluate the correlation functions. Figures 4(a) and 4(b) shows R_H and S as a function of the strength of the AF order m_{AF} and the vertical stripe v, respectively. The temperature is fixed at $0.02t/k_B$. As mentioned above, the region near the left axis in Fig. 4(b) shows that S is once suppressed by the weak stripe, i.e., $|v|\sim|v_c|$. Then both are remarkably suppressed when m_{AF} and v are comparable with each other, i.e., near the diagonal line. Figures 5(a)–5(c) show the equal-energy contours and Fermi surfaces for the three points in Figs. 4(a) and 4(b). Especially, Fig. 5(b) belongs to the nontrivial case and shows the peculiar shape of the Fermi surface. According to Ref. 30, σ_{xy} could be reduced in the nontrivial Fermi surface compared to that of the circular Fermi surface surrounding the same size of area in $\vec{k}$ space. Especially when the Fermi surface has both parts of positive convexity and negative one, this reduction would be very effective as seen in the region $|v|\sim|m_{AF}|$.

Finally, the effects of the AF order and the vertical (horizontal) stripe on the temperature dependences of R_H and S are shown in Figs. 3(a) and 3(b). The AF order enhances both the quantities almost over the whole temperature range except for the region near the peak of R_H, and shift the peaks to a higher temperature. This is because the AF order introduces the additional energy scale, i.e., the band gap. Then the vertical (horizontal) stripe remarkably suppresses both R_H and S in the whole temperature range when v is comparable with m_{AF}. These results are parallel to the above results where the temperature is fixed.

V. DISCUSSION

Now we discuss the above results in comparison with the experiments. The most important issue is whether the high-temperature phase above T_N and the pseudogap region can be described in terms of the massless Dirac fermions by putting $m_{AF}=0$. The temperature and x dependences of R_H and S appear to be qualitatively consistent with the experiments. However, when one looks at the x dependence of the conductivity σ_{xx} at $T=300$ K above T_N, it fits better with $\propto x^{3/2}$ rather than $\propto x$ due to the x dependence of the hole mobility.[7] On the other hand, $\sigma_{xx}\propto\sqrt{x}$ and $\sigma_{xy}\propto x^0$ in our model, which

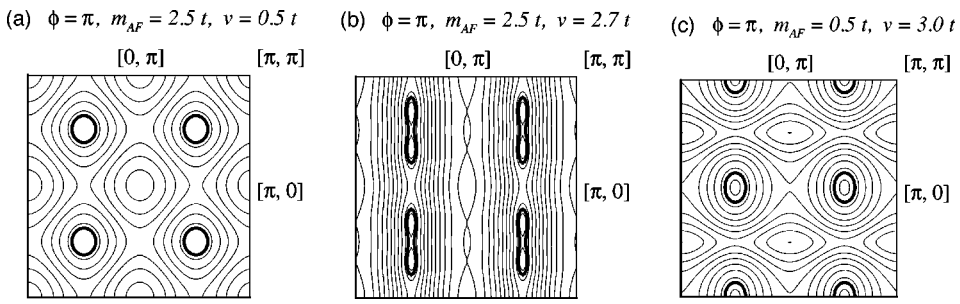

FIG. 5. Schematic view of the energy contours for three parameter sets. Thick lines in each figure represent the Fermi surface for $x=0.02$. The reduced Brillouin zone is the square with the corners $[\pm\pi/2,\pm\pi/2]$. Copies are also drawn over the original Brillouin zone for $\phi=m_{AF}=v=0$.

is contradicting the above experiments. Furthermore, the onset of the AF order at T_N does not affect the conductivity σ_{xx} in the experiment,[7] which is more difficult to understand from any mean-field picture. This is related to the interpretation of the insulating gap at $x=0$. In the mean-field picture, it is due to the AF ordering while there remains a large gap even without the AF order in the Mott insulator picture. If the large gap disappears and crossing of the two bands occurs above T_N, the upper band becomes relevant at around $T_x \cong J\sqrt{x}$ and particle-hole symmetry will be recovered above T_x. This massless Dirac spectrum also gives the x dependence as described above. Therefore it seems that the x dependence observed in experiments suggests that the Mott insulating picture is more appropriate for the high-temperature phase. In other words, the Dirac fermion without the AF gap is never relevant to the underdoped cuprates. This is also consistent with the asymmetry of ARPES between hole-doped[2] and electron-doped[34] cuprates. Recent experiments on NCCO[34] strongly suggest that the minima of the electron dispersion are at $\vec{k}=(\pi,0)$ and $(0,\pi)$, and the particle-hole symmetry is broken. This appears to be consistent with the SDW picture with appropriate longer-range hopping integrals t' and t''. However, the sign of t' and t'' is reversed when one consider the t-t'-t''-J model for the electron-doped case, and the minimum at $(\pi,0)$ is recovered by self-consistent Born approximation,[16] and its results can be interpreted as the flux state with the AF order.[35] Therefore, it makes sense to consider the flux state together with the AF order, but not without it.

The AF ordered state, on the other hand, can be well described in terms of the mean-field state with the flux order. In this AF state, the conventional behavior of the doped carriers is expected without the stripe formation. Therefore the effects of the stripes are the most interesting issue. It is found that $R_H = a^2/(|e|x)$ is a rather robust feature at low temperatures. The suppression occurs only when the AF order and the vertical (horizontal) stripe coexist, and the directional average is taken within the plane. The thermopower is also suppressed by the stripe formation, and does not need the directional average. The difference between Ref. 6 and Ref. 7 seems to be due to the sample preparation. A longer time annealing has been done for the former case, while the sample is quenched in the latter case. Therefore it is expected that the chain is more ordered in the former case, which might help the stripe formation. The fourfold symmetry observed in the magnetoresistance[36] is interpreted to be due to the induced stripe in terms of the in-plane external magnetic field.

In conclusions, we have studied the transport properties of the flux state as a model for underdoped cuprates. This model shows several remarkable features such as parity anomaly, scaling laws for R_H and S, the recovery of particle-hole symmetry at high temperatures. Compared with the existing experimental data, in particular, the x dependence of σ_{xx}, it is unlikely that this model describes the underdoped cuprates without the AF order. However, the flux state with the AF order, which gives the mass gap to the Dirac fermions, describes well the ordered state. In this case, the stripe order affects the transport properties in a nontrivial way, and we have discussed the experiments from this view point.

ACKNOWLEDGMENTS

The authors would like to acknowledge fruitful discussions with Y. Ando, C. M. Ho, T. K. Lee, S. Miyasaka, T. Okuda, N. P. Ong, Y. Tokura, and S. Uchida. N.N. was supported by Priority Areas Grants and Grant-in-Aid for COE research from the Ministry of Education, Science, Culture and Sports of Japan.

APPENDIX A: CONDUCTIVITY IN THE CONTINUUM MODEL

This appendix is devoted to present the uniform conductivity $\sigma_{\mu\nu}(\omega)$ of the continuum effective theory constructed in Sec. II. When the effect of the relaxation is approximated by replacing ω by $\Omega=\omega+i/\tau$ with the lifetime τ and we can diagonalize a given Hamiltonian, the linear-response theory generally gives the following representation for the uniform conductivity:

$$\sigma_{\mu\nu}(\Omega)=ie^2\sum_{\alpha,\beta}\frac{f_F(\epsilon_\beta-\mu)-f_F(\epsilon_\alpha-\mu)}{\epsilon_\alpha-\epsilon_\beta}\times\frac{\langle\alpha|J_\nu|\beta\rangle\langle\beta|J_\mu|\alpha\rangle}{\Omega+\epsilon_\beta-\epsilon_\alpha}, \tag{A1}$$

where α and β are the quantum indices of eigen states, J_μ represents μ component of the current density, and $f_F(\epsilon-\mu)$ is the Fermi distribution function. We apply the above formula to the effective theory in Sec. II, i.e. (2+1)D Dirac fermions in the external magnetic field. For example, in the case of the contribution from sector 1 with σ spin, the following replacements are sufficient:

$$\sum_{\alpha,\beta}\to\frac{|eB|}{2\pi}\sum_{n,n'=0}^{\infty}\sum_{s,s'=\pm},\quad |\alpha\rangle\to|n\sigma\pm\rangle,\quad \epsilon_\alpha\to\pm\epsilon_{n\sigma},$$

$$J_x\to\hat{j}_x=2ta\tau_1, \tag{A2}$$

$$J_y\to\hat{j}_y=2ta\left(\cos\frac{\phi}{2}\tau_1+\sin\frac{\phi}{2}\tau_2\right).$$

Here $|n\sigma\pm\rangle$ and ϵ_n are defined by Eqs. (8)–(11) in Sec. II. τ_i are the Pauli matrices in the space of $|\tilde{\uparrow}(\tilde{\downarrow})\rangle$. [See Eq. (8).] Then the contribution from sector 1 with σ spin is represented by

$$\sigma^{1\sigma}_{\mu\nu}(\Omega)=ie^2\frac{|eB|}{2\pi}\sum_{n,n'=0}^{\infty}\sum_{s,s'=\pm}\frac{f_F(s'\epsilon_{n'\sigma}-\mu)-f_F(s\epsilon_{n\sigma}-\mu)}{s\epsilon_{n\sigma}-s'\epsilon_{n'\sigma}}\frac{\langle n\sigma s|\hat{j}_\nu|n'\sigma s'\rangle\langle n'\sigma s'|\hat{j}_\mu|n\sigma s\rangle}{\Omega+s'\epsilon_{n'\sigma}-s\epsilon_{n\sigma}}$$

$$=ie^2\frac{|eB|}{2\pi}\sum_{n,n'=0}^{\infty}\sum_{s=\pm}\left[\frac{1}{\epsilon_{n'\sigma}+\epsilon_{n\sigma}}\frac{\langle n\sigma s|\hat{j}_\nu|n'\sigma -s\rangle\langle n'\sigma -s|\hat{j}_\mu|n\sigma s\rangle}{\Omega-s(\epsilon_{n'\sigma}+\epsilon_{n\sigma})}\right.$$

$$+\frac{f_F(\epsilon_{n'\sigma}-s\mu)-f_F(\epsilon_{n\sigma}-s\mu)}{\epsilon_{n\sigma}-\epsilon_{n'\sigma}}\frac{\langle n\sigma s|\hat{j}_\nu|n'\sigma s\rangle\langle n'\sigma s|\hat{j}_\mu|n\sigma s\rangle}{\Omega+s(\epsilon_{n'\sigma}-\epsilon_{n\sigma})}$$

$$\left.-\frac{f_F(\epsilon_{n'\sigma}+s\mu)-f_F(\epsilon_{n\sigma}-s\mu)}{\epsilon_{n\sigma}+\epsilon_{n'\sigma}}\frac{\langle n\sigma s|\hat{j}_\nu|n'\sigma -s\rangle\langle n'\sigma -s|\hat{j}_\mu|n\sigma s\rangle}{\Omega-s(\epsilon_{n'\sigma}+\epsilon_{n\sigma})}\right]$$

$$=ie^2\frac{|eB|}{2\pi}\sum_{n,n'=0}^{\infty}\sum_{s=\pm}\left[\frac{2f_F(\epsilon_{n\sigma}-s\mu)-1}{\Omega^2-(\epsilon_{n'\sigma}+\epsilon_{n\sigma})^2}\left\{\frac{(-i\Omega)\mathrm{Re}[\langle n\sigma s|\hat{j}_\nu|n'\sigma -s\rangle\langle n'\sigma -s|\hat{j}_\mu|n\sigma s\rangle]}{\epsilon_{n'\sigma}+\epsilon_{n\sigma}}\right.\right.$$

$$\left.+s\,\mathrm{Im}[\langle n\sigma s|\hat{j}_\nu|n'\sigma -s\rangle\langle n'\sigma -s|\hat{j}_\mu|n\sigma s\rangle]\right\}+\frac{2f_F(\epsilon_{n\sigma}-s\mu)}{\Omega^2-(\epsilon_{n'\sigma}-\epsilon_{n\sigma})^2}$$

$$\left.\times\left\{\frac{(-i\Omega)\mathrm{Re}[\langle n\sigma s|\hat{j}_\nu|n'\sigma s\rangle\langle n'\sigma s|\hat{j}_\mu|n\sigma s\rangle]}{\epsilon_{n\sigma}-\epsilon_{n'\sigma}}+s\,\mathrm{Im}[\langle n\sigma s|\hat{j}_\nu|n'\sigma s\rangle\langle n'\sigma s|\hat{j}_\mu|n\sigma s\rangle]\right\}\right]. \tag{A3}$$

It is noted that all distribution functions in the first equality represent those of electrons. In the second equality, we have done the transformation $f_F(-\epsilon-\mu)\to 1-f_F(\epsilon+\mu)$ for negative-energy modes in order to change the distribution function of the valence band to that of the quasihole. In the third equality, the difference of distribution functions is pulled apart to each distribution function. This procedure is justified because $\langle n\sigma s|\hat{j}_\mu|n'\sigma s'\rangle\neq 0$ only for $n'=n\pm 1$ as we will see below and the distribution function $f_F(\epsilon_{n\sigma}\pm\mu)$ decreases sufficiently fast as n increases.

The final procedure is to substitute the matrix elements by the following explicit forms:

$$\langle n\sigma\pm|\tau_1|n'\sigma\pm\rangle=\pm\frac{1}{2}\left[\sqrt{\frac{E_{n\sigma\pm}E_{n+1\sigma\mp}}{\epsilon_{n\sigma}\epsilon_{n+1\sigma}}}\delta_{n+1,n'}+\sqrt{\frac{E_{n'+1\sigma\mp}E_{n'\sigma\pm}}{\epsilon_{n'+1\sigma}\epsilon_{n'\sigma}}}\delta_{n,n'+1}\right],$$

$$\langle n\sigma\pm|\tau_1|n'\sigma\mp\rangle=\mp\frac{1}{2}\left[\sqrt{\frac{E_{n\sigma\pm}E_{n+1\sigma\pm}}{\epsilon_{n\sigma}\epsilon_{n+1\sigma}}}\delta_{n+1,n'}-\sqrt{\frac{E_{n'+1\sigma\mp}E_{n'\sigma\mp}}{\epsilon_{n'+1\sigma}\epsilon_{n'\sigma}}}\delta_{n,n'+1}\right],$$

$$\langle n\sigma\pm|\tau_2|n'\sigma\pm\rangle=\mp i\,\mathrm{sgn}(eB_\phi)\frac{1}{2}\left[\sqrt{\frac{E_{n\sigma\pm}E_{n+1\sigma\mp}}{\epsilon_{n\sigma}\epsilon_{n+1\sigma}}}\delta_{n+1,n'}-\sqrt{\frac{E_{n'+1\sigma\mp}E_{n'\sigma\pm}}{\epsilon_{n'+1\sigma}\epsilon_{n'\sigma}}}\delta_{n,n'+1}\right],$$

$$\langle n\sigma\pm|\tau_2|n'\sigma\mp\rangle=\pm i\,\mathrm{sgn}(eB_\phi)\frac{1}{2}\left[\sqrt{\frac{E_{n\sigma\pm}E_{n+1\sigma\pm}}{\epsilon_{n\sigma}\epsilon_{n+1\sigma}}}\delta_{n+1,n'}+\sqrt{\frac{E_{n'+1\sigma\mp}E_{n'\sigma\mp}}{\epsilon_{n'+1\sigma}\epsilon_{n'\sigma}}}\delta_{n,n'+1}\right], \tag{A4}$$

where $E_{n\sigma\pm}=\epsilon_{n\sigma}\pm\mathrm{sgn}(eB_\phi)u_\sigma$. (The absence of one of zero modes is appropriately represented by $E_{n\sigma\pm}$.) As for the dc conductivity, the contribution from sector 1 with σ spin is given by

$$\sigma^{1\sigma}_{xx}=\frac{e^2}{2\pi}\tau^{-1}K^2_{eB}\sum_{s=\pm}\left\{f_F(|u_\sigma|-s\mu)\frac{|u_\sigma|[1+\mathrm{sgn}(su_\sigma eB_\phi)]}{(K^2_{eB_\phi}+\tau^{-2})^2+4\tau^{-2}u^2_\sigma}+\sum_{n=1}f_F(\epsilon_n-s\mu)\right.$$

$$\times[(K^4_{eB_\phi}-\tau^{-4})^2+8(K^4_{eB_\phi}+\tau^{-4})\tau^{-2}\epsilon^2_n+(4\tau^{-2}\epsilon^2_n)^2]^{-1}[\tau^{-2}(\tau^{-2}+4\epsilon^2_n)(\epsilon_n+u^2_\sigma\epsilon^{-1}_n)$$

$$\left.+K^4_{eB_\phi}(3\epsilon_n-u^2_\sigma\epsilon^{-1}_n)-4K^2_{eB_\phi}\tau^{-2}|u_\sigma|\mathrm{sgn}(su_\sigma eB_\phi)]\right\}+\frac{e^2}{2\pi}\frac{\tau^{-1}K^2_{eB}}{2}$$

$$\times\sum_{n=0}^{\infty}\frac{1}{(\epsilon_n+\epsilon_{n+1})[\tau^{-2}+(\epsilon_n+\epsilon_{n+1})^2]}\left(1+\frac{u^2_\sigma}{\epsilon_n\epsilon_{n+1}}\right), \tag{A5}$$

$$\sigma_{xy}^{1\sigma}=\frac{e^2}{2\pi}\mathrm{sgn}(eB)K_{eB_\phi}^2\sum_{s=\pm}\left\{\frac{s}{2}f_F(|u_\sigma|-s\mu)\frac{(K_{eB_\phi}^2+\tau^{-2})[1+\mathrm{sgn}(su_\sigma eB_\phi)]}{(K_{eB_\phi}^2+\tau^{-2})^2+4\tau^{-2}u_\sigma^2}\right.$$

$$+\sum_{n=1}sf_F(\epsilon_n-s\mu)[(K_{eB_\phi}^4-\tau^{-4})^2+8(K_{eB_\phi}^4+\tau^{-4})\tau^{-2}\epsilon_n^2+(4\tau^{-2}\epsilon_n^2)^2]^{-1}[K_{eB_\phi}^2(K_{eB_\phi}^4-\tau^{-4}+4\tau^{-2}u_\sigma^2)$$

$$\left.+\tau^{-2}(K_{eB_\phi}^4-\tau^{-4}+4\tau^{-2}\epsilon_n^2)|u_\sigma|\epsilon_n^{-1}\,\mathrm{sgn}(su_\sigma eB_\phi)]\right\}$$

$$-\frac{e^2}{2\pi}\mathrm{sgn}\left(\sin\frac{\phi}{2}\right)\frac{K_{eB_\phi}^2}{2}\sum_{n=0}^{\infty}\frac{u_\sigma(\epsilon_n+\epsilon_{n+1})}{\epsilon_n\epsilon_{n+1}[\tau^{-2}+(\epsilon_n+\epsilon_{n+1})^2]}+\sigma_{xx}^{1\sigma}\cos\frac{\phi}{2},\tag{A6}$$

The terms without the distribution function represent the parts of the interband effect, which remain even in the case $\mu=0$ and $k_BT=0$. As for $\sigma_{xx}^{1\sigma}$, the contribution from the interband effect is negligible in the semiclassical limit ($K_{eB_\phi}\ll 1\ll|\mu|\tau$) compared to the contribution from the Fermi level. In this case, the Boltzmann theory is a good approximation. (The interband effect is neglected in the Boltzmann theory.) On the other hand, as for $\sigma_{xy}^{1\sigma}$, the last two terms, which include the interband effect remaining in the case $\mu=0$ and $k_BT=0$, cancel out after summing up the contribution from all sectors. In other words, when the parity symmetry is breaking, i.e., the numbers of right and left Dirac fermions are unbalanced, we cannot neglect the remaining interband effect. Especially in the case $\tau=\infty$ and $B\to 0$, the last line but one in $\sigma_{xy}^{1\sigma}$ gives a contribution $\pm 1/2$ in the unit e^2/h as long as $u_\sigma\neq 0$, where the sign depends on u_σ and ϕ, and h is Planck's constant. However, it is noted that the total σ_{xy} should take a integer value in the unit e^2/h when it is quantized. Therefore, in the case where this interband effect is crucial, we must seriously consider the contribution from the bottom of valence bands and the top of conduction bonds, which are beyond the range of the continuum model.

APPENDIX B: TEMPERATURE DEPENDENCE OF THE CHEMICAL POTENTIAL

Here we consider the temperature dependence of the chemical potential μ in the limit $B\to 0$. When there is no stripe formation, the doping parameter of the continuum model is given by

$$-x=d_s\sum_{c=\pm}\sum_{s=\pm}\int\frac{d^2p}{(2\pi)^2}sf_F(\epsilon_c(\vec{p})-s\mu)$$

$$=\frac{d_f}{8\pi t^2\left|\sin\frac{\phi}{2}\right|}\sum_{s=\pm}\int_{|m_{AF}|}^{\infty}d\epsilon\epsilon sf_F(\epsilon-s\mu).\tag{B1}$$

Here d_s is the number of spin degrees of freedom, i.e., $d_s=2$, d_f is the total number of inner degrees of freedom, i.e., $d_f=(\mathrm{left}+\mathrm{right})\times d_s=4$, and

$$\epsilon_\pm(\vec{p})=\sqrt{(2ta)^2\left(p^2\pm 2\cos\frac{\phi}{2}p_xp_y\right)+m_{AF}^2}.\tag{B2}$$

The sign of x is taken as it is positive when $\mu<0$.

In the low-temperature approximation, $k_BT\ll(|\mu|-|m_{AF}|)$, we can estimate the right-hand side of Eq. (B1) by using the sharpness of the Fermi distribution function as follows:

$$-x=\frac{d_f}{16\pi t^2}\mathrm{sgn}(\mu)\,\theta(|\mu|-|m_{AF}|)$$

$$\times\left[\mu^2-m_{AF}^2+\frac{\pi^2}{3}(k_BT)^2+\cdots\right].\tag{B3}$$

Then, in the hole-doping case, i.e. $\mu<-|m_{AF}|$, the temperature dependence of μ is given by

$$|\mu|\cong\sqrt{4\pi xt^2\left|\sin\frac{\phi}{2}\right|+m_{AF}^2-\frac{\pi^2}{3}(k_BT)^2},\tag{B4}$$

where we have used $d_f=4$.

On the other hand, in the high-temperature approximation, $k_BT\gg|\mu|$, we can estimate the right-hand side of Eq. (B1) as follows:

$$-x=\frac{d_f}{8\pi t^2\left|\sin\frac{\phi}{2}\right|}\sum_{s=\pm}\frac{1}{\beta^2}\int_{\beta|m_{AF}|}^{\infty}dy\frac{sy}{1+e^{y-s\beta\mu}},$$

$$=\frac{d_f}{4\pi t^2\left|\sin\frac{\phi}{2}\right|}\frac{\mu}{\beta}\left[\frac{\beta|m_{AF}|}{1+e^{\beta|m_{AF}|}}+\ln(1+e^{-\beta|m_{AF}|})+\cdots\right],\tag{B5}$$

where $\beta=1/(k_BT)$ and we have expanded the integrand in $\beta\mu$. Finally, in the hole-doping case, i.e., $\mu<0$, the temperature dependence of μ is given by

$$|\mu| \cong \frac{\pi x t^2 \beta \left|\sin\frac{\phi}{2}\right|}{\frac{\beta|m_{AF}|}{1+e^{\beta|m_{AF}|}} + \ln(1+e^{-\beta|m_{AF}|})}, \tag{B6}$$

where $d_f=4$ is substituted. It is noted that, fixing the doping parameter and the temperature, the above formula is a increasing function of $|m_{AF}|$. Therefore, the AF order m_{AF} suppresses the recovery of the particle-hole symmetry.

APPENDIX C: SCALING LAWS OF R_H AND S

In this appendix, we present the derivation of the scaling laws of R_H and S in the case of $m_{AF}=m_{\rm diag}=v=0$ and in the limit $B\to 0$. In order to see the temperature dependence of the Fermi distribution function $f_F(\xi)$, we introduce the function $f(\beta\xi)=f_F(\xi)$ where $\beta=1/(k_BT)$. Then, from Eq. (B1) with $m_{AF}=0$, the doping parameter x is given by the following equation:

$$-x = \frac{1}{2\pi t^2\left|\sin\frac{\phi}{2}\right|}\sum_{s=\pm}\int_0^\infty d\epsilon\epsilon s f(\beta(\epsilon - s\mu))$$

$$= \frac{1}{2\pi t^2\left|\sin\frac{\phi}{2}\right|}\sum_{s=\pm}\frac{1}{\beta^2}\int_0^\infty dy y s f(y-s\beta\mu), \tag{C1}$$

It is easy to see that $t\sqrt{x}/(k_BT)$ is represented by a function of $\mu/(k_BT)$. Therefore, when we can consider the inverse of the function, $\mu/(k_BT)$ is represented by a function of $t\sqrt{x}/(k_BT)$.

In the same way, by making the energy integral dimensionless, the response functions are represented as

$$\sigma_{xx} \cong \frac{e^2}{2\pi\left|\sin\frac{\phi}{2}\right|}\left(\frac{2\tau}{\beta}\right) \times \sum_{s=\pm}\int_0^\infty dy\left[-y\frac{df}{dy}(y-s\beta\mu) + \left(\frac{1}{2}-f(y-s\beta\mu)\right)\frac{1}{1+\left(\frac{2\tau}{\beta}y\right)^2}\right], \tag{C2}$$

$$\sigma_{xy} \cong \frac{e^2}{2\pi}\left|\sin\frac{\phi}{2}\right|\frac{2a^2eB}{x}(\beta t\sqrt{x})^2\left(\frac{2\tau}{\beta}\right)^2 \times \sum_{s=\pm}\int_0^\infty dy s\left[-\frac{df}{dy}(y-s\beta\mu)\right]\left[1+\frac{1}{1+\left(\frac{2\tau}{\beta}y\right)^2}\right], \tag{C3}$$

$$\beta\sigma_{xx}^Q \cong \frac{e}{2\pi\left|\sin\frac{\phi}{2}\right|}\left(\frac{2\tau}{\beta}\right) \times \sum_{s=\pm}\int_0^\infty dy\left[-sy(y-s\beta\mu)\frac{df}{dy}(y-s\beta\mu) - \left(\frac{1}{2}-f(y-s\beta\mu)\right)\frac{\beta\mu}{1+\left(\frac{2\tau}{\beta}y\right)^2}\right], \tag{C4}$$

where $\sigma_{\mu\nu}^Q$ is the response function given by the correlation function of the electric current density $e\vec{J}$ and the heat current density $\vec{J}^Q$. In the first-quantized representation, the heat current density for sector 1 with σ spin is given by

$$\hat{j}_x^Q = (2ta)^2\left(\hat{p}_x + \cos\frac{\phi}{2}\hat{p}_y\right) - \mu\hat{j}_x, \tag{C5}$$

$$\hat{j}_y^Q = (2ta)^2\left(\hat{p}_y + \cos\frac{\phi}{2}\hat{p}_x\right) - \mu\hat{j}_y. \tag{C6}$$

This is the continuum version of the heat current density derived in the lattice model, which is presented in Appendix D. The right-hand side of each response function is a function of $t\sqrt{x}/(k_BT)$ and τk_BT, because $\mu/(k_BT)$ is a function of $t\sqrt{x}/(k_BT)$. Therefore, $xR_H \cong x\sigma_{xy}/(B\sigma_{xx}^2)$ and $S \cong \sigma_{xx}^Q/(T\sigma_{xx})$ are functions of $t\sqrt{x}/(k_BT)$ and τk_BT. In the semiclassical limit, the dependence of τk_BT is negligible, and xR_H and S scale as functions of $t\sqrt{x}/(k_BT)$.

APPENDIX D: HEAT CURRENT DENSITY IN THE LATTICE MODEL

The definition of the heat current density is not straightforward as against that of the electric current density. Here we present the heat current density of the system represented by Eq. (1). The Hamiltonian is rewritten as $H=\Sigma_{\vec{r}}h_{\vec{r}}$, where

$$h_{\vec{r}} = \frac{1}{2}\sum_{\hat{\delta},\sigma}\left[-t_{\vec{r}+\hat{\delta},\vec{r}}c_{\vec{r}+\hat{\delta},\sigma}^\dagger c_{\vec{r}\sigma} - t_{\vec{r}+\hat{\delta},\vec{r}}^* c_{\vec{r}\sigma}^\dagger c_{\vec{r}+\hat{\delta},\sigma}\right] + \sum_\sigma (V_{\vec{r}\sigma}-\mu)c_{\vec{r}\sigma}^\dagger c_{\vec{r}\sigma}, \tag{D1}$$

$$V_{\vec{r}\sigma} = -[u_\sigma\cos(\vec{Q}\cdot\vec{r}) + v\cos(\vec{Q}_v\cdot\vec{r})], \tag{D2}$$

and the sum of the unit vector $\hat{\delta}$ runs $\pm\hat{x}$ and $\pm\hat{y}$. It is clear that $h_{\vec{r}}$ is interpreted as a local heat density. The heat current density would be conceptually defined by averaging the product of the local velocity and $h_{\vec{r}}$. However, it is difficult to define the local velocity, especially in the second-quantized formalism. Here we define the heat current density from the analogy with the conceptual definition. First, using $h_{\vec{r}}$, we introduce the quantity $\vec{R}$ as follows, $\vec{R}=V^{-1}\Sigma_{\vec{r}}\vec{r}h_{\vec{r}}$, where V is the volume (area) of the system. This quantity has

the dimension of heat density multiplied by length. Then, we define the heat current density as a time derivative of $\vec{R}$, i.e., $\vec{J}^Q = i[H,\vec{R}]$. From the dimension of $\vec{R}$, $\vec{J}^Q$ correctly has the dimension of heat current density. Finally, the explicit form of $\vec{J}^Q$ is given by

$$\vec{J}^Q = \vec{J}^E - \mu \vec{J}, \tag{D3}$$

$$\begin{aligned}\vec{J}^E = \frac{1}{V}\sum_{\vec{r}} \Bigg[& -\frac{i}{2}\sum_{\hat{\delta},\hat{\delta}',\sigma} (\hat{\delta}+\hat{\delta}') t_{\vec{r}+\hat{\delta},\vec{r}} t^*_{\vec{r}+\hat{\delta},\vec{r}} c^\dagger_{\vec{r}+\hat{\delta}+\hat{\delta}',\sigma} c_{\vec{r}\sigma} \\ & + \frac{i}{2}\sum_{\hat{\delta},\sigma} \hat{\delta}(V_{\vec{r}+\hat{\delta}} + V_{\vec{r}}) t_{\vec{r}+\hat{\delta},\vec{r}} c^\dagger_{\vec{r}+\hat{\delta},\sigma} c_{\vec{r}\sigma} \Bigg], \\ = \frac{1}{V}\sum_{\vec{k},\sigma} \Bigg[& \sum_{\hat{\mu}=\hat{x},\hat{y}} (-4t^2)\hat{\mu} \sin k_\mu \Bigg\{ \cos k_\mu \\ & + \cos\frac{\phi}{2}\cos(\epsilon_{\mu\nu}k_\nu) \Bigg\} c^\dagger_{\vec{k}\sigma} c_{\vec{k}\sigma} + 2vt\hat{y}\sin k_y \\ & \times \Bigg\{ -\cos\frac{\phi}{4} c^\dagger_{\vec{k}\sigma} c_{\vec{k}+\vec{Q}_x,\sigma} + i\sin\frac{\phi}{4} c^\dagger_{\vec{k}\sigma} c_{\vec{k}+\vec{Q}_y,\sigma} \Bigg\} \Bigg], \end{aligned} \tag{D4}$$

$$\begin{aligned}\vec{J} &= \frac{i}{V}\sum_{\vec{r}}\sum_{\hat{\delta},\sigma} \hat{\delta} t_{\vec{r}+\hat{\delta},\vec{r}} c^\dagger_{\vec{r}+\hat{\delta},\sigma} c_{\vec{r}\sigma} \\ &= \frac{1}{V}\sum_{\vec{k},\sigma}\sum_{\hat{\mu}=\hat{x},\hat{y}} 2t\hat{\mu}\sin k_\mu \Bigg[\cos\frac{\phi}{4} c^\dagger_{\vec{k}\sigma} c_{\vec{k}\sigma} \\ &\quad + (-1)^\mu i \sin\frac{\phi}{4} c^\dagger_{\vec{k}\sigma} c_{\vec{k}+\vec{Q},\sigma} \Bigg], \end{aligned} \tag{D5}$$

where $\vec{Q}=(\pi,\pi)$, $\vec{Q}_x=(\pi,0)$, and $\vec{Q}_y=(0,\pi)$. The symbol $(-1)^\mu$ means that $(-1)^x=1$ and $(-1)^y=-1$. In a physical sense, $\vec{J}^E$ is the energy current density, and $\vec{J}$ is the current density.

As for the continuum limit, the following transformation of bases is performed before taking the limit.

$$\begin{bmatrix} c_{\vec{k}\sigma} \\ c_{\vec{k}+\vec{Q},\sigma} \\ c_{\vec{k}+\vec{Q}_x,\sigma} \\ c_{\vec{k}+\vec{Q}_y,\sigma} \end{bmatrix} = \begin{bmatrix} U_+ & O \\ O & U_- \end{bmatrix} \begin{bmatrix} \psi_{\vec{k},1\sigma} \\ \psi_{\vec{k},2\sigma} \end{bmatrix}, \tag{D6}$$

where $\psi_{\vec{k},i\sigma}$ $(i=1,2)$ is a two-component operator, and

$$U_\pm = \frac{1}{\sqrt{2}}(\tau_3 \pm \tau_1)\left(\cos\frac{\phi}{8}\tau_1 \pm \sin\frac{\phi}{8}\tau_2\right). \tag{D7}$$

When there is no stripe, $\psi_{\vec{k},i\sigma}$ with $\vec{k}\sim(\pi/2,\pi/2)$ corresponds to the Dirac fermion of i sector $(i=1,2)$ with σ spin.

APPENDIX E: R_H IN THE CASE $|v|<|v_C|$

Here we present the analysis of R_H when two lower bands are doped. Around the tops of these two bands, their dispersions are approximated as

$$\epsilon_\pm(\vec{p}) = -\sqrt{(2ta)^2 p_x^2 + (2\tilde{t}_\pm a)^2 p_y^2 + \tilde{m}_\pm}, \tag{E1}$$

where $\tilde{t}_\pm = t\sqrt{1\pm|v/m_{AF}|}$ and $\tilde{m}_\pm = |m_{AF}|\pm|v|$. In this case, by considering the two bands separately and then adding the contributions at the stage of conductivity, we can get the Hall coefficient $R_H \cong a^2/(|e|x)$ at a low temperature, where x is the total doping parameter. However, when there are domains of stripes with different directions, we should take an average of conductivity tensor. Then, we obtain the following result:

$$R_H \cong \frac{a^2}{|e|}\frac{4\left[x-\left|\frac{v}{m_{AF}}\right|(x_- - x_+)\right]}{\left[2x-\left|\frac{v}{m_{AF}}\right|(x_- - x_+)\right]^2}, \tag{E2}$$

where x_+ and x_- are doping parameters for the first and second bands, respectively. Then, from the conservation of the total doping x and the commonness of the chemical potential μ, x_+ and x_- are determined using the following equations:

$$x_- + x_+ = x, \tag{E3}$$

$$x_-\sqrt{1-\left|\frac{v}{m_{AF}}\right|} - x_+\sqrt{1+\left|\frac{v}{m_{AF}}\right|} = \frac{|v m_{AF}|}{2\pi t^2}. \tag{E4}$$

It is noted here that $x_\pm$ includes the contribution of both spin degrees of freedom. When $|v|$ is larger than the critical value $|v_c|$, i.e.,

$$\begin{aligned}|v|>|v_c| = |m_{AF}|\left(\frac{\sqrt{2\pi x}t}{m_{AF}}\right)^2 \Bigg[& \sqrt{1+\frac{1}{4}\left(\frac{\sqrt{2\pi x}t}{m_{AF}}\right)^4} \\ & - \frac{1}{2}\left(\frac{\sqrt{2\pi x}t}{m_{AF}}\right)^2 \Bigg], \end{aligned} \tag{E5}$$

only the second band is doped, i.e., $x_+=0$ and $x_-=x$.

We can also analyze the thermopower S in a similar way. However, its expression is more complicated than that of R_H and is not suggestive. Therefore, we do not give the explicit analysis, but point out that, in the region $0<|v|<|v_c|$, S is highly reduced when $|v|$ increases as shown in Fig. 4(b).

*Electronic address: m.onoda@aist.go.jp
†Electronic address: nagaosa@appi.t.u-tokyo.ac.jp

[1] J. D. Reger and A. P. Young, Phys. Rev. B **37**, 5978 (1988); S. Chakravarty, B. I. Halperin, and D. R. Nelson, Phys. Rev. Lett. **60**, 1057 (1988).
[2] D. S. Marshall, D. S. Dessau, A. G. Loeser, C.-H. Park, A. Y. Matsuura, J. N. Eckstein, I. Bozovic, P. Fournier, A. Kapitulnik, W. E. Spicer, and Z.-X. Shen, Phys. Rev. Lett. **76**, 4841 (1996); M. Norman, H. Ding, M. Rnderia, J. C. Campuzano, Y. Yokoya, T. Takeuchi, T. Takahasi, T. Mochiku, K. Kadowaki, P. Guptasarma, and D. G. Hinks, Nature (London) **392**, 157 (1998); F. Ronning, C. Kim, D. L. Feng, D. S. Marshall, A. G.

Loeser, L. L. Miller, J. N. Eckstein, I. Bozovic, and Z.-X. Shen, Science **282**, 2067 (1998).
[3] N. P. Ong, Z. Z. Wang, J. Clayhold, J. M. Tarascon, L. H. Greene, and W. R. McKinnon, Phys. Rev. B **35**, 8807 (1987); M. Suzuki, *ibid.* **39**, 2312 (1989); T. Nishikawa, J. Takeda, and M. Sato, J. Phys. Soc. Jpn. **62**, 2568 (1993); H. Y. Hwang, B. Batlogg, H. Takagi, H. L. Kao, Kwo , R. J. Cava, J. J. Krajewski, and W. F. Peck, Jr., Phys. Rev. Lett. **72**, 2636 (1994).
[4] H. Takagi, B. Batlogg, H. L. Kao, J. Kwo, R. J. Cava, J. J. Krajewski, and W. F. Peck, Jr., Phys. Rev. Lett. **69**, 2975 (1992).
[5] T. Ito, K. Takenaka, and S. Uchida, Phys. Rev. Lett. **70**, 3995 (1993).
[6] Y. Wang and N. P. Ong, Proc. Natl. Acad. Sci. U.S.A. **98**, 11 091 (2001).
[7] Y. Ando, A. N. Lavrov, S. Komiya, K. Segawa, and X. F. Sun, Phys. Rev. Lett. **87**, 017001 (2001).
[8] Y. Ando and K. Segawa, cond-mat/0108053 (unpublished); cond-mat/0110487 (unpublished).
[9] J. R. Schrieffer, X. G. Wen, and S. C. Zhang, Phys. Rev. B **39**, 11 663 (1989).
[10] I. Affleck and J. B. Marston, Phys. Rev. B **37**, 3774 (1988); J. B. Marston and I. Affleck, *ibid.* **39**, 11 538 (1988); P. Lederer, D. Poilblanc, and T. M. Rice, Phys. Rev. Lett. **63**, 1519 (1989); F. C. Zhang, *ibid.* **64**, 974 (1990); T. C. Hsu, J. B. Marston, and I. Affleck, Phys. Rev. B **43**, 2866 (1991).
[11] P. W. Anderson, Science **235**, 1196 (1987); P. W. Anderson, G. Baskaran, Z. Zou, and T. Hsu, Phys. Rev. Lett. **58**, 2790 (1987).
[12] G. Kotliar, Phys. Rev. B **37**, 3664 (1988); G. Kotliar and J. Liu, *ibid.* **38**, 5142 (1988).
[13] Y. Suzumura, Y. Hasegawa, and H. Fukuyama, J. Phys. Soc. Jpn. **57**, 2768 (1988).
[14] I. Affleck, Z. Zou, T. Hsu, and P. W. Anderson, Phys. Rev. B **38**, 745 (1988).
[15] T. C. Hsu, Phys. Rev. B **41**, 11 379 (1990); C. M. Ho, V. N. Muthukumar, M. Ogata, and P. W. Anderson, Phys. Rev. Lett. **86**, 1626 (2001).
[16] C. L. Kane, P. A. Lee, and N. Read, Phys. Rev. B **39**, 6880 (1989); F. Marsiglio, A. E. Ruckenstein, S. Schmitt-Rink, and C. M. Varma, *ibid.* **43**, 10 882 (1991); T. Xiang and J. M. Wheatley, *ibid.* **54**, R12 653 (1996).
[17] E. Dagotto, A. Nazarenko, and M. Boninsegni, Phys. Rev. Lett. **73**, 728 (1994); T. Tohyama, Y. Shibata, S. Maekawa, Z.-X. Shen, N. Nagaosa, and L. L. Miller, J. Phys. Soc. Jpn. **69**, 9 (2000).
[18] R. B. Laughlin, Phys. Rev. Lett. **79**, 1726 (1997).
[19] T. K. Lee and C. T. Shih, Phys. Rev. B **55**, 5983 (1997).
[20] H. Matsukawa and H. Fukuyama, J. Phys. Soc. Jpn. **61**, 1882 (1992); M. Inaba, H. Matsukawa, M. Saitoh, and H. Fukuyama, Physica C **257**, 299 (1996).
[21] X. G. Wen and P. A. Lee, Phys. Rev. Lett. **76**, 503 (1996); P. A. Lee, N. Nagaosa, T. K. Ng, and X. G. Wen, Phys. Rev. B **57**, 6003 (1998).
[22] S. Chakravarty, R. B. Laughlin, D. K. Morr, and C. Nayak, Phys. Rev. B **63**, 094503 (2001).
[23] T. Noda, H. Eisaki, and S. Uchida, Science **286**, 265 (1999).
[24] S. Uchida (private communication).
[25] N. Nagaosa and P. A. Lee, Phys. Rev. B **43**, 1233 (1991).
[26] S. Deser, R. Jackiw, and S. Templeton, Phys. Rev. Lett. **48**, 975 (1982).
[27] L. P. Gorkov and J. R. Schrieffer, Phys. Rev. Lett. **80**, 3360 (1998); S. H. Simon and P. A. Lee, *ibid.* **78**, 1548 (1997); M. Franz and Z. Tesanovic, *ibid.* **84**, 554 (2000).
[28] H. B. Nielsen and M. Ninomiya, Phys. Lett. **130B**, 389 (1983).
[29] J. D. Lykken, J. Sonnenschein, and N. Weiss, Phys. Rev. D **42**, 2161 (1995); V. Zeitlin, Phys. Lett. B **352**, 422 (1995); T. Ito and T. Sato, *ibid.* **367**, 290 (1996); T. Ito and H. Kato, Nucl. Phys. B **551**, 723 (1999).
[30] N. P. Ong, Phys. Rev. B **43**, 193 (1991).
[31] G. D. Mahan, Solid State Phys. **51**, 81 (1998).
[32] J. M. Tranquada, B. J. Stemlieb, J. D. Axe, Y. Nakamura, and S. Uchida, Nature (London) **375**, 561 (1995).
[33] P. Prelovsek, T. Tohyama, and S. Maekawa, Phys. Rev. B **64**, 052512 (2001).
[34] N. P. Armitage, D. H. Lu, C. Kim, A. Damascelli, K. M. Shen, F. Ronning, D. L. Feng, P. Bogdanov, Z.-X. Shen, Y. Onose, Y. Taguchi, Y. Tokura, P. K. Mang, N. Kaneko, and M. Green, Phys. Rev. Lett. **87**, 147003 (2001); (unpublished).
[35] T. K. Lee, C. M. Ho, and N. Nagaosa (unpublished).
[36] Y. Ando, A. N. Lavrov, and K. Segawa, Phys. Rev. Lett. **83**, 2813 (1999).